FREQUENCY STABILITY OF MASER OSCILLATORS OPERATED WITH ENHANCED CAVITY Q

Michel Têtu and Pierre Tremblay
Laboratoire de Recherches sur les Oscillateurs et Systèmes
Université Laval, Québec, Canada

and

Paul Lesage, Pierre Petit and Claude Audoin
Laboratoire de l'Horloge Atomique
Université de Paris-Sud, Orsay, France

ABSTRACT

This paper presents an experimental study of the short term frequency stability of masers equipped with an external feedback loop to increase the cavity quality factor. The frequency stability of a hydrogen and a rubidium maser are measured and compared with theoretical evaluation. It is observed that the frequency stability passes through an optimum when the cavity Q is varied. Long term fluctuations are discussed and the optimum mid term frequency stability achievable by small size active and passive H-masers is considered.

INTRODUCTION

Much effort has been devoted recently to hydrogen masers in order to reduce their size, their weight, and to increase their long term frequency stability. New technology and design improvements applied to conventional masers [1] led to the relization of the most stable atomic frequency standards in the mid term region of averaging time [2], and to a sufficiently light and rugged device to be space-borne [3]. Small size masers with various types of microwave cavities were proposed and tested [4,5]. Masers with dielectric loaded cavities operated as passive frequency standards were also investigated [6,7]. The latest development is a small cavity oscillating maser, equipped with an external loop to enhance the quality factor [8,9].

A theoretical model, established to evaluate the amplitude noise and the phase noise in actively and passively operated masers [10,11] made possible the prediction of the short term frequency stability of a maser equipped with an external feedback loop [12]. Subsequently, the ultimate performance of such a device were evaluated and compared to the corresponding passive standard [13]. The following gives an experimental check of that theory applied to a hydrogen maser and a rubidium maser of conventional design [14,15],so equipped.

THEORY

The time domain frequency stability of an oscillator is expressed by the two sample variance of the relative frequency fluctuations over an averaging time τ, with no dead time (Allan variance) [16]. In the case of a maser, the dominant frequency fluctuations considered arise from both the thermal noise within the electromagnetic cavity and the thermal noise added in the receiver necessary to detect the signal [17]. When the spectrum of the fluctuations is limited by a low-pass filter of cut-off frequency f_c, it can be shown [15,18] that the short term frequency stability, in the time domain, is expressed by the relation:

$$\sigma_y^2(\tau) = \frac{4k\theta_c}{P_0} \left\{ \frac{3\pi f_c}{2\omega_0^2} \left[1 + (F_r - 1) \frac{Q_{ext}}{Q_c} \frac{\theta_r}{\theta_c} \right] \frac{1}{\tau^2} + \frac{1}{8Q_\ell^2} \frac{1}{\tau} \right\} \quad , \qquad (1)$$

where k is the Boltzmann constant, θ_c, Q_c and Q_{ext} are respectively the temperature, the loaded and the external quality factors of the cavity, θ_r and F_r are the temperature and the noise factor of the receiver, ω_0 is the maser angular frequency, Q_ℓ is the atomic line Q and P_0 is the power delivered to the cavity by the atoms.

The first two terms of equation (1) come from the thermal noise added to the maser signal by the cavity and the receiver respectively; they correspond to white phase noise. The third term is white frequency noise resulting from the stimulated emission of radiation by the cavity's thermal noise within the atomic linewidth. The atomic power can be expressed simply, in terms of the cavity Q, by the folling [19]:

$$P_0 = \frac{1}{2} S \hbar \omega_0 \frac{Q_c - Q_t}{Q_c} \qquad (2)$$

where S is a flux term, $\hbar$ is the Planck constant divided by 2π and Q_t is a threshold Q value determined by various maser parameters.

A feedback loop, external to the cavity, can be utilized to increase the quality factor; a schematic diagram is given in figure 1. Part of the maser signal is taken out, amplified and re-injected into the cavity. If the phase of the injected signal is properly adjusted, it will add to the signal already in the cavity, thus simulating a lower loss cavity. In this set-up, the cavity is used in transmission, with coupling loop coefficients β_1 and β_2 at the injection and output ports respectively. The loaded cavity Q becomes [20]:

$$Q_c = \frac{Q_0}{1 + \beta_1 + \beta_2} \qquad (3)$$

where Q_0 is the unloaded cavity Q associated with ohmic losses. Two external cavity Q's are defined as follows:

$$Q_{ext,1} = \frac{Q_0}{\beta_1} \quad \text{and} \quad Q_{ext,2} = \frac{Q_0}{\beta_2} \tag{4}$$

The enhanced cavity Q has a maximum value given by:

$$Q_e = \frac{Q_0}{1+\beta_1+\beta_2-2G\sqrt{\beta_1\beta_2}} \tag{5}$$

where G is the total voltage gain of the feedback loop. The atomic power of such a maser will now be:

$$P_0 = \frac{1}{2} S\hbar\omega_0 \frac{Q_e - Q_t}{Q_e} \tag{6}$$

The presence of the feedback loop alters the thermal noise within the cavity. Part of the cavity noise undergoes the same process as the maser signal and the loop amplifier adds a certain amount of thermal noise. These supplementary contributions give to the cavity an effective noise temperature which can be written [21]:

$$T_c = \theta_c \frac{Q_e}{Q_c}\left[1+\beta_1(F_a-1)G^2\frac{Q_c}{Q_0}\frac{\theta_a}{\theta_c}\right] \tag{7}$$

where θ_a and F_a are the temperature and the noise figure of the loop amplifier.

If we substitute equations (3), (4), (5), (6) and (7) into equation (1), we obtain for the time domain short term frequency stability of a maser equipped with an external feedback loop, an expression of the form:

$$\sigma^2(\tau) = K_{-2}\tau^{-2} + K_{-1}\tau^{-1} \tag{8}$$

where the white phase noise contribution is:

$$K_{-2} = \frac{12\pi k\theta_r f_c}{S\hbar\omega_0^3}\frac{Q_e}{(Q_e-Q_t)}\left\{\frac{\theta_c}{\theta_r}\frac{Q_e}{Q_0}\left[1+\beta_1+\beta_2+\right.\right.$$

$$\left.\left.\frac{\theta_a}{\theta_c}(F_a-1)\frac{1}{4\beta_2}\left[1+\beta_2+\beta_2-\left(\frac{Q_0}{Q_e}\right)^2\right]\right]+(F_r-1)\frac{1+\beta_1+\beta_2}{\beta_2}\right\} \tag{9}$$

and the white frequency noise contribution is:

$$K_{-1} = \frac{k\theta_c}{S\hbar\omega_0 Q_\ell^2} \frac{Q_e^2}{(Q_e - Q_t)} \frac{1}{Q_0}\left[1+\beta_1+\beta_2+\frac{\theta_a}{\theta_c}(F_a-1)\frac{1}{4\beta_2}\left(1+\beta_1+\beta_2-\frac{Q_0}{Q_e}\right)^2\right] \quad (10)$$

These equations are explicitly expressed in terms of the fixed cavity parameters β_1, β_2 and Q_0 and its enhanced Q.

Computation of equation (8) with the parameters given in table 1 for a conventional H-maser and a conventional Rb-maser yields the results shown in figure 2.

	H-maser	Rb-maser
ω_0	$2\pi(1.42\times10^9)$ rad/sec	$2\pi(6.83\times10^9)$ rad/sec
Q_ℓ	2.2×10^9	5.5×10^7
S (normalization parameter)	7.15×10^{11} at./sec	3.65×10^{15} ph./sec
Q_t	40 000	22 500
Q_0	64 400	28 000
β_1	0.157	0.60
β_2	0.171	0.55
θ_c	300 K	337 K
$F_r = F_a$	1.78	2.24
θ_r	293 K	290 K
θ_a	300 K	290 K
f_c	5 Hz	50 Hz

Table 1: Maser parameters used to evaluate equation (8).

The behavior of the two types of noise is drawn from the two asymptotical lines obtained for the very short averaging times and for the long averaging times respectively.

EXPERIMENTAL STUDIES

In order to verify the model just described, both an hydrogen and a rubidium maser were equipped with a feedback loop as illustrated in figure 1. The cavity Q was varied by changing the value of the attenuator and measured with the usual technique of the r.f. pulse decay [19]. For the

H-maser phase of the loop was adjusted, at each attenuator setting to cause no frequency shift from non-enhanced operation. In the case of the Rb-maser, the phase was adjusted to make the output power maximum.

The short term frequency stability for various values of Q_e with the parameters shown in table 1 are given in figure 3. It is observed that the stability decreases when the cavity Q reaches high values. In the case of the Rb-maser, a roll-over is observed in the very short term region (τ <.02 sec). In both systems, unpredicted sources of instabilities dominate for long averaging times. The solid lines are best fit polynomials.

From the coefficient of the polynomials we can extrapolate the white phase noise contribution, K_{-2}, and the white frequency noise contribution, K_{-1}. The square root of each contribution is shown in figure 4. The solid lines are the result of the evaluation of equations (9) and (10) as a function of Q_e. They are normalized with the flux term, S, so that the $\sqrt{K_{-2}}$ curve passes over the experimental point indicated by an arrow. These results are experimental evidence that each noise contribution can be minimized by choosing the proper value for Q_e. Consequently, if the overall frequency stability is to be optimized, the Q_e value will be selected according to the averaging time considered.

A comparison between the experimental observation and the theoretical evaluation of the frequency stability at different averaging times, as functions of the enhanced Q, is given in figure 5. We see that the stability is optimum for a certain value, Q_e^{opt}. This value depends slightly on the averaging time chosen since the dominant type of noise evolves from the white phase noise to the white frequency noise when the averaging time is varied from very short term to mid term. In this last comparison, the averaging time was limited to values smaller than 300 sec for the H-maser and .07 sec for the Rb-maser in order to reduce the influence of the long term instabilities.

In figure 3 frequency instabilities other than the ones predicted by equation (8), are evident. Since their contribution increases with the cavity Q, we are tempted to relate them to a cavity pulling effect. We measured the relative frequency shift due to temperature variation of the feedback loop components for different cavity Q's. The results are given in figure 6 for each maser. The coefficients are approximately 1×10^{-13}/°C at 40 000 for the H-maser and 3×10^{-11}/°C at 25 000 for the Rb-maser. These shifts are due to a phase pulling effect related to a change in the length of the feedback loop and explain some of the long term instabilities. It is seen from these measurements that a very precise control of the loop temperature will be necessary if high performance is required. Automatic cavity tuning such as the fast auto-tuning system [7,22] would then improve the long term

frequency stability of masers actively operated with an external feedback loop.

SMALL SIZE HYDROGEN MASER

The theoretical model seems to fit well the reality observed. We will now use it to predict the ultimate frequency stability achievable by small size active H-maser with enhanced cavity Q. To do so, the maser parameters found in equation (8) are expressed in terms of more fundamental parameters which are associated with the gain and linewidth of the atomic system. They are the spin exchange parameter [1]:

$$q = \frac{\sigma \bar{v}_r \hbar}{2\mu_0 \mu_B} \frac{T_b}{T_t} \frac{1}{V_b} \frac{V_c}{\eta Q_c} \frac{I_{tot}}{I} \tag{11}$$

and the threshold flux:

$$I_{th} = \frac{\hbar}{\mu_0 \mu_B^2} \frac{V_c}{\eta Q_c} \frac{1}{T_t^2} \tag{12}$$

In these equations I_{tot} is the total atomic flux entering the bulb, I is that portion of the flux in the upper active quantum state, μ_0 is the magnetic permeability of vacuum, μ_B is the Bohr magneton, η is the filling factor, V_c is the cavity volume, σ is the spin exchange cross-section, $\bar{v}_r$ the relative average hydrogen velocity, T_b is the bulb storage time constant, V_b is the bulb volume and $T_t = \sqrt{T_1^0 T_2^0}$ with T_1^0 and T_2^0 the longitudinal and transversal relaxation time constants.

Considering only the effect of the white frequency noise contribution, it has been shown [13, eq. 44] that the frequency stability of an active maser, with enhanced cavity Q, is expressed by the relation:

$$\sigma_{a,e}^2(\tau) = \frac{4kT}{\hbar^2 \omega_0^3} \mu_0 \mu_B^2 \frac{\eta Q_c}{V_c} \left(\frac{Q_e}{Q_c}\right)^2 H_{a,e}\left(q, \frac{I}{I_{th}}\right) \frac{1}{\tau} \tag{13}$$

The function $H_{a,e}(q, I/I_{th})$ [13, eq. 17] has to be minimized in order to reach the ultimate frequency stability. If the parameters of currently existing small size masers are substituted in equation (13), we obtain:

$$\sigma_{a,e,opt}^2(\tau) \simeq 0.6 \times 10^{-26} \tau^{-1}$$

The same approach can be applied to the case of a passive H-maser. One can show [13, eq. 25] that the optimum frequency stability is expressed by:

$$\sigma_p^2(\tau) = \frac{4kT}{\hbar^2\omega_0^3}\,\mu_0\mu_B^2\,\frac{\eta Q_c}{V_c}\,H_p\left(q\,,\frac{I}{I_{th}}\right)\frac{1}{\tau} \qquad (14)$$

Here again the function $H_p(q,I/I_{th})$ must be minimized by a proper choice of q and I/I_{th}. When evaluating equation (14) with the parameters of existing passive masers [13, table 1] we have the value:

$$\sigma^2_{p,op}(\tau) \simeq 3.6 \times 10^{-26}\tau^{-1}$$

Both types of small size H-masers have then approximately the same ultimate frequency stability in the mid term region.

CONCLUSION

This experimental study as well as the previous one on amplitude noise [11] give great confidence in the theoretical model developed to consider the effect of thermal noise on the amplitude and the phase of actively or passively operated masers. When a maser is operated with a feedback loop to enhance the cavity Q, an optimum is found where the frequency stability is best. Small size H-masers of the same design can then be operated either actively or passively; they will offer about the same mid term frequency stability when all the parameters are optimized. Automatic cavity tuning is needed on both devices to improve the long term stability: the electronic complexity will then be of the same level.

REFERENCES

[1] D. Kleppner, H.C. Berg, S.B. Crampton, N.F. Ramsey, R.F.C. Vessot, H.E. Peters and J. Vanier, "Hydrogen Maser Principles and Techniques", Phys. Rev., Vol. 138, No 4A, A972-A983, 1965.

[2] R.F.C. Vessot, M.W. Levine and E.M. Mattison, "Comparison of Theoretical and Observed Hydrogen Maser Stability Limitation due to Thermal Noise and the Prospect for Improvement by Low-Temperature Operation", Proc. Ninth Annual Precise Time and Time Interval (PTTI) Applications and Planning Meeting, pp. 549-569, Washington, D.C., 1978.

[3] R.F.C. Vessot, M.W. Levine, E.M. Mattison, T.E. Hoffman, E.A. Imbier, M. Têtu, G. Nystrom, J.J. Kelt, Jr., H.F. Trucks and J.L. Vaniman, "Space-Borne Hydrogen Maser Design", Proc. Eighth Annual Precise Time and Time Interval (PTTI) Applications and Planning Meeting, pp. 277-333, Washington, D.C., 1978.

[4] E.M. Mattison, M.W. Levine, R.F.C. Vessot, "New TE_{111}-Mode Hydrogen Maser", Proc. Eighth Annual Precise Time and Time Interval (PTTI) Applications and Planning Meeting, pp. 355-380, Washington, D.C., 1978.

[5] H.E. Peters, "Small, Very Small, and Extremely Small Hydrogen Masers", Proc. 32nd Annual Symposium on Frequency Control, pp. 469-476, 1978.

[6] F.L. Walls and H. Hellwig, "A New Kind of Passively Operating Hydrogen Frequency Standards", Proc. 30th Annual Symposium on Frequency Control, pp. 473-480, 1976.

[7] D.A. Howe, F.L. Walls, H.E. Bell, H. Hellwig, "A Small Passively Operated Hydrogen Maser", Proc. 33rd Annual Symposium on Frequency Control, pp. 554-562, 1979.

[8] H.T.M. Wang, "An Oscillating Compact Hydrogen Maser", Proc. 34th Annual Symposium on Frequency Control, pp. 364-369, 1980.

[9] H.E. Peters, "Feasibility of Extremely Small Hydrogen Masers", Proc. 35th Annual Symposium on Frequency Control, to be published.

[10] P. Lesage, C. Audoin and M. Têtu, "Amplitude Noise in Passively and Actively Operated Masers", Proc. 33rd Annual Symposium on Frequency Control, pp. 515-535, 1979.

[11] P. Lesage, C. Audoin, M. Têtu, "Measurement of the Effect of Thermal Noise on the Amplitude of Oscillation of a Maser Oscillator", IEEE Trans. Instrum. Meas., Vol. IM-29, No 4, pp. 311-316, 1980.

[12] P. Lesage and C. Audoin, "Frequency Stability of an Oscillating Maser: Analysis of the Effect of an External Feedback Loop", IEEE Trans. Instrum. Meas., Vol. IM-30, No 3, pp. 182-186, 1981.

[13] C. Audoin, J. Viennet and P. Lesage, "Hydrogen Maser: Active or Passive?", Proc. 3rd Symposium on Frequency Standards and Metrology, Aussois, France, to be published, 1981.

[14] P. Petit, J. Viennet, R. Barillet, M. Desaintfuscien and C. Audoin, "Hydrogen Maser Design at the Laboratoire de l'Horloge Atomique", Proc. Eighth Annual Precise Time and Time Interval (PTTI) Applications and Planning Meeting, pp. 229-247, Washington, D.C., 1976.

[15] M. Têtu, G. Busca and J. Vanier, "Short Term Frequency Stability of the Rb^{87} Maser", IEEE Trans. Instrum. Meas., Vol. IM-22, No 3, pp. 250-257, 1973.

[16] J.A. Barnes, A.R. Chi, L.S. Cutler, D.J. Healey, D.B. Leeson, T.E. McGunigal, J.A. Mullen, W.L. Smith, R.L. Sydnor, R.F.C. Vessot and G.M.R. Winkler, "Characterization of Frequency Stability", IEEE Trans. Instrum. Meas., Vol. IM-20, No 2, pp. 105-120, 1971.

[17] L.S. Cutler, "Coulomb Corrections to Inelastic Electron Scattering and Maser Oscillator Thermal Noise Analysis", Ph.D. thesis, Stanford University, 1966, unpublished.

[18] P. Lesage and C. Audoin, "Effect of Dead-Time on the Estimation of the Two-Sample Variance", IEEE Trans. Instrum. Meas., Vol. IM-28, No 1, pp. 6-10, 1979.

[19] C. Audoin, "Le maser à hydrogène en régime transitoire", D.Sc. thesis, Université de Paris-Sud à Orsay, 1967, unpublished.

[20] G. Boudouris, "Cavités électromagnétiques", Dunod, Paris, 1971.

[21] P. Lesage, "Caractérisation des fluctuations de fréquence et analyse du bruit d'amplitude dans le maser à hydrogène", D.Sc. thesis, Université de Paris-Sud à Orsay, 1980, unpublished.

[22] C. Audoin, "Fast Cavity Auto-Tuning Systems for Hydrogen Masers", Revue de Physique Appliquée, Vol. 16, p. 125, 1981.

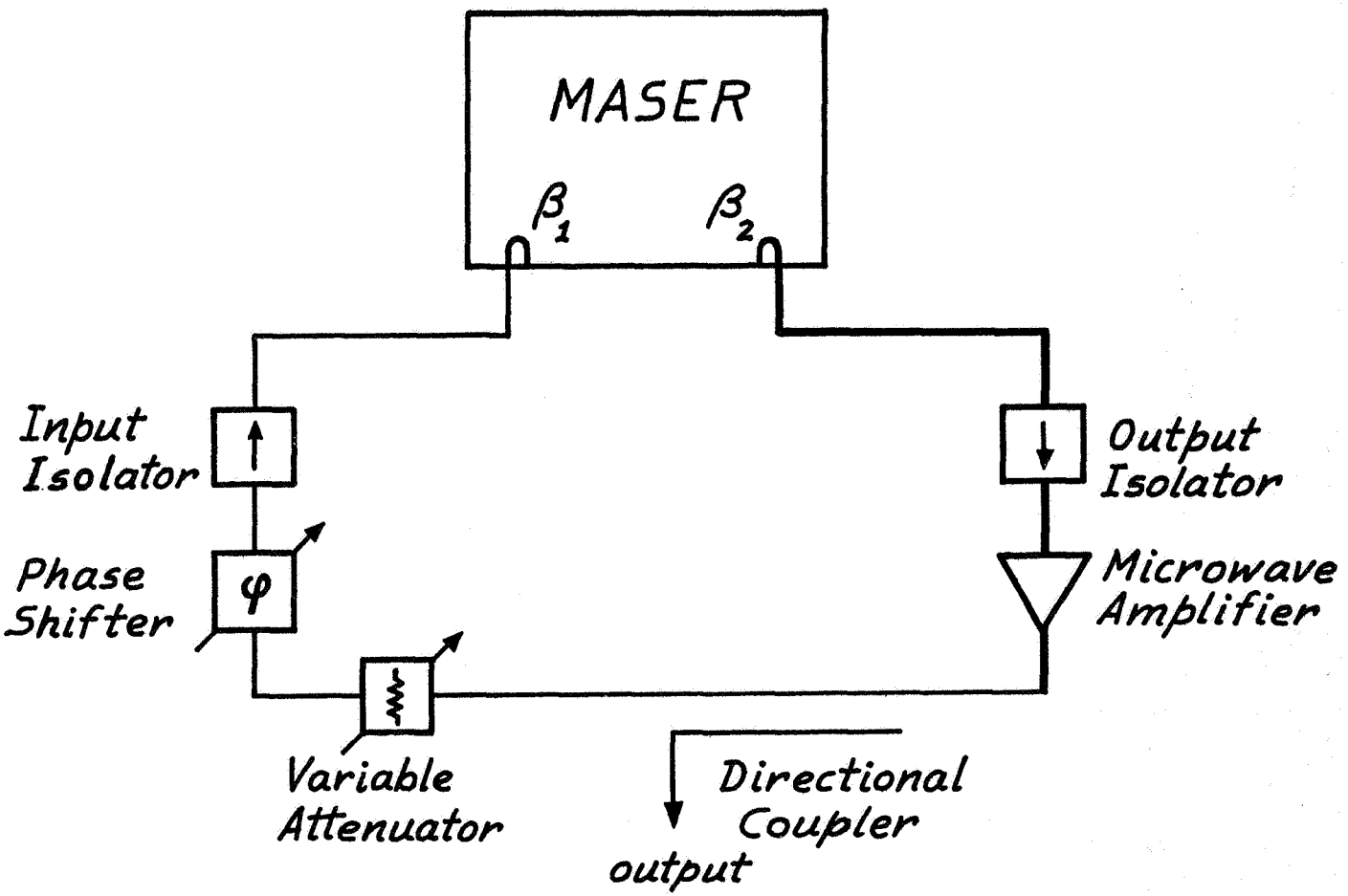

Fig. 1 Schematic diagram of the feedback loop associated with a maser cavity.

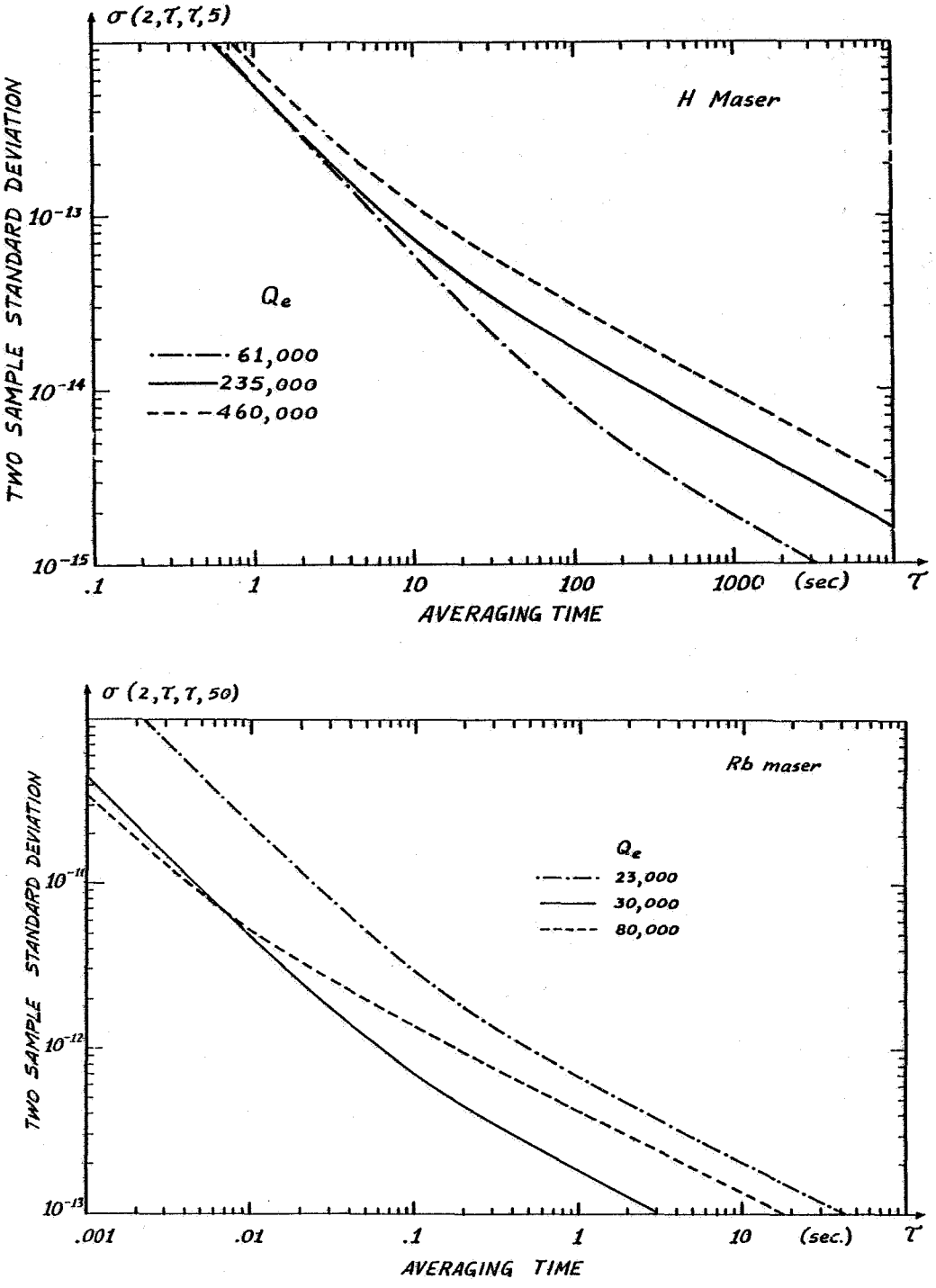

Fig. 2 Short term frequency stability: theoretical evaluation.

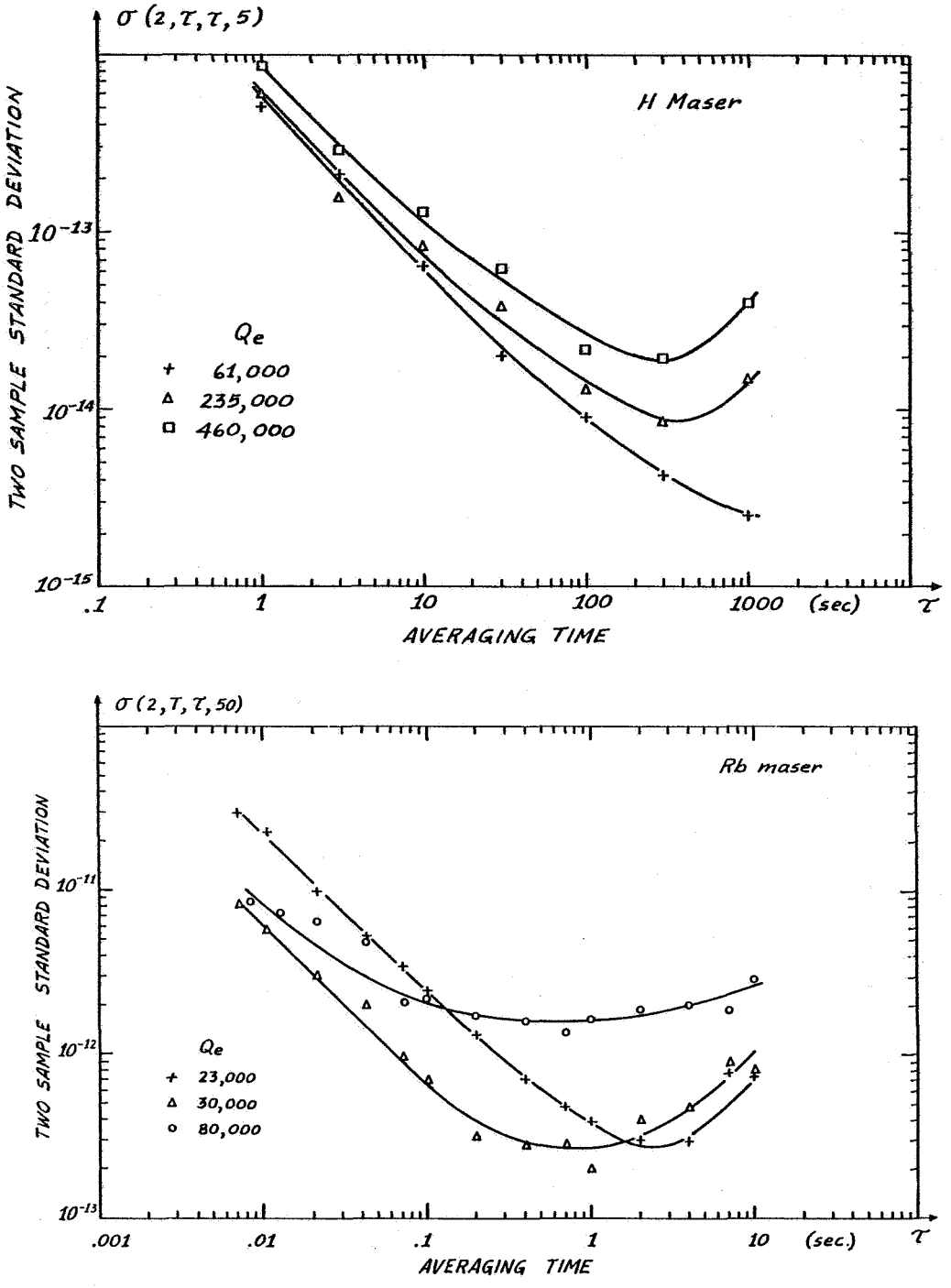

Fig. 3 Short term frequency stability: measurement.

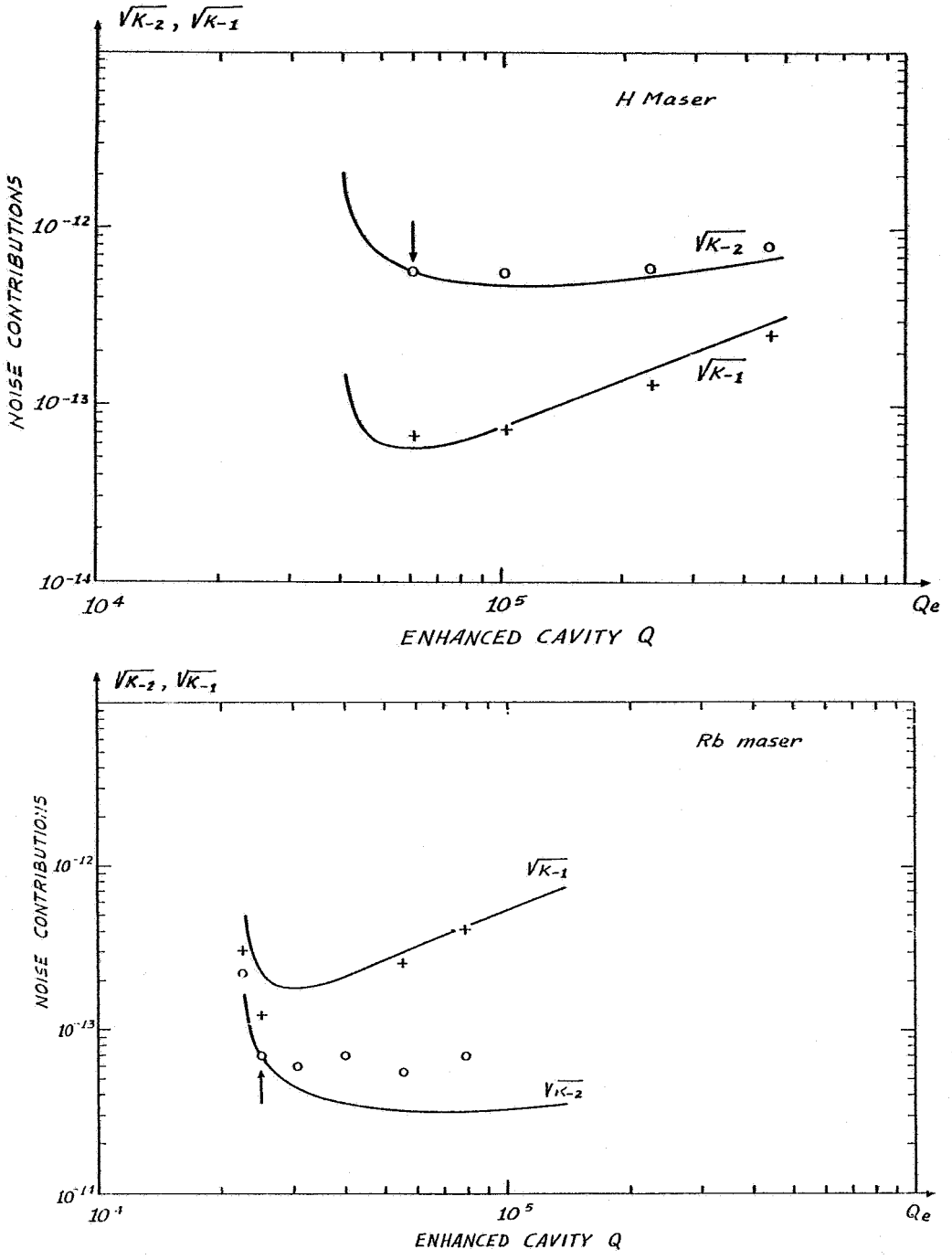

Fig. 4 White phase noise and white frequency noise contributions.

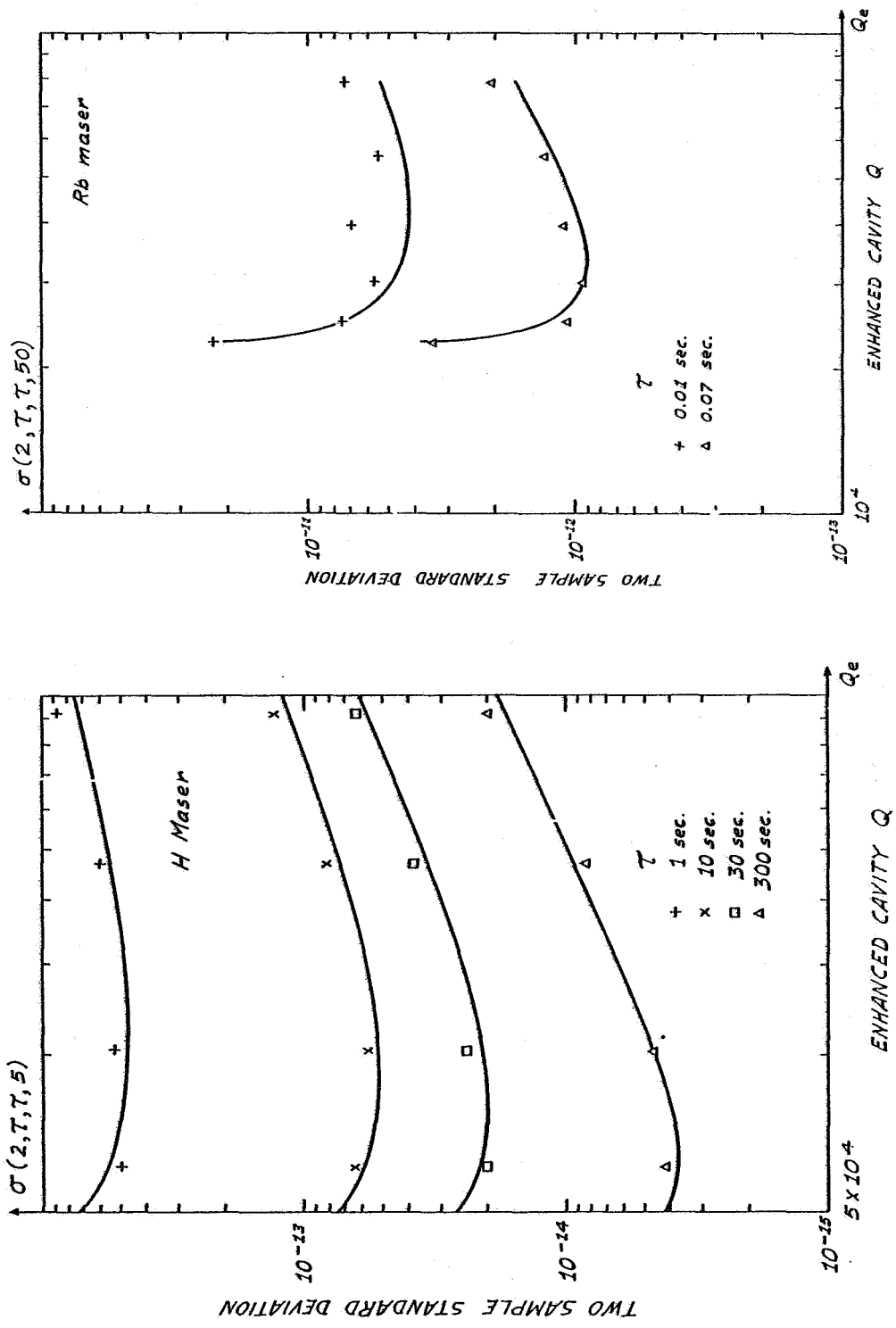

Fig. 5 Overall short term frequency stability.

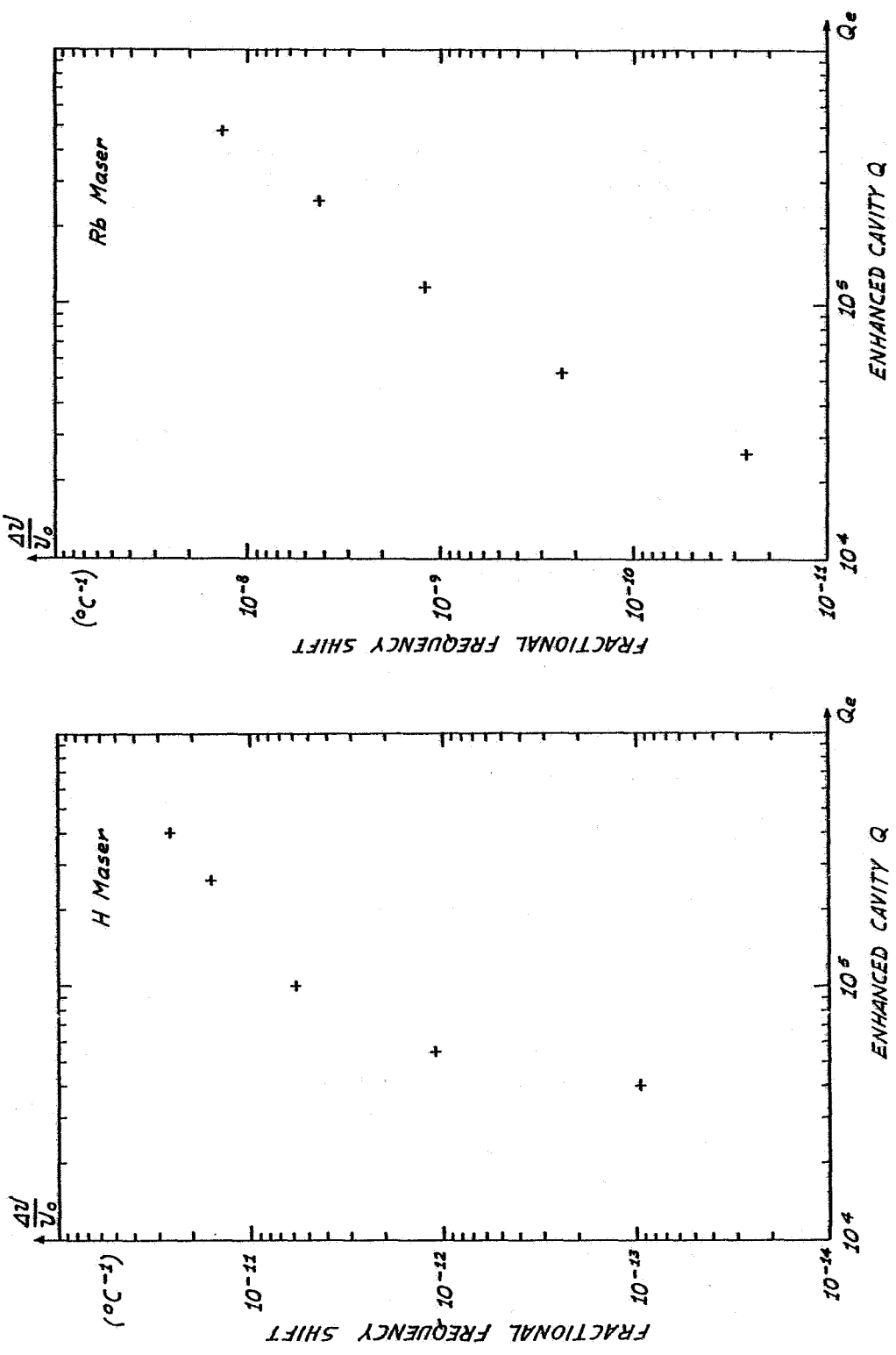

Fig. 6 Relative maser frequency shift associated to a variation of 1 °C of the loop temperature.